Coastal Engineering 82 (2013) 9–24

Contents lists available at ScienceDirect

Coastal Engineering

journal homepage: www.elsevier.com/locate/coastaleng

Modelling an anthropogenic effect of a tidal basin evolution applying tidal and wave boundary forcings: Ley Bay, East Frisian Wadden Sea

Pushpa Dissanayake *[,1], Andreas Wurpts [2]

Coastal Research Station, Lower Saxony Water Management, Coastal Defence and Nature Conservation Agency, An der Mühle 5, D-26548 Norderney, Germany

ARTICLE INFO

Article history:
Received 4 March 2013
Received in revised form 18 July 2013
Accepted 10 August 2013
Available online 4 September 2013

Keywords:
Anthropogenic effect
Ley Bay
Leyhörn
Sediment transport formula
Wave schematization
Long-term morphological evolution
Delft3D
East Frisian Wadden Sea

ABSTRACT

Potential physical impacts of an anthropogenic effect on a tidal basin evolution are investigated applying the Delft3D model suite under both tidal and wave boundary forcings. Study area is based on a peninsula construction of the Ley Bay in the East Frisian Wadden Sea. Model simulation spans from 1975 to 1990 in two stages of which the second stage begins with the implemented peninsula on the 1984 predicted morphology. The model bed consists of initially distributed three sediment fractions. Sensitivity of the Ley Bay evolution is analysed under three different sediment transport formulations: 1) Van Rijn, 1993 (*VR93*), 2) Soulsby, 1997 (*SVR*) and 3) Van Rijn et al., 2004 (*VR04*).

Offshore tides and waves are transformed up to the model boundaries via a nested modelling approach and a statistically derived highly schematised wave climate is adopted in the simulations. Predicted morphologies indicate lower agreement with the measured morphology due to including very sparse data. Despite this discrepancy, they reproduce the major changes in the Ley Bay caused by the peninsula construction while each formula results in a slightly different channel/shoal pattern. Predicted evolution under the *SVR* shows the strongest sediment exporting system and therefore the lowest agreement with the 1990 measured morphology. Both *VR93* and *VR04* formulas resulted in marginal exporting systems and more or less similar morphologies. In fact, only the *VR04* prediction indicates a fair agreement with the 1990 data. Temporal evolution under the *VR04* shows concentrated velocity patterns at the bay entrance and in the eastward bay channel resulting in the development of this channel and sedimentation in the southern part of the bay as found in the data.

1. Introduction

Anthropogenic effects such as diking, land reclamation, peat-cutting and damming of channels since the Middle Ages have shown a great influence on the present-day morphology of the Wadden Sea tidal basin systems. Reinforcing of the existing dunes to serve as dikes, construction of jetties and closing of the tidal basins (e.g. Zuider Sea (Thijsse, 1972; Elias et al., 2003)) have also resulted in major impacts on the Wadden Sea evolution. Some of these human interventions are found in the Eastern part of the Wadden Sea (i.e. East Frisian Wadden Sea), e.g. Ley Bay, Harle Bay, Jade Bay etc. (Homeier et al., 2010). The approach discussed here uses a coupled numerical model to investigate the morphological evolution of the Ley Bay during a 15 year period (from 1975 to 1990) including the effect of the peninsula construction '*Leyhörn*'.

The *Leyhörn* peninsula has been constructed in 1984 and its main functions are coastal safety, navigational access and inland drainage. Efficiency of these functions is directly related to the morphological set-up of the Ley Bay area. Strong morphological changes are inevitable because the *Leyhörn* peninsula interrupts the existing system. As such, a better insight of the potential bed changes of the bay is required to develop effective and efficient planning and management strategies. The overarching aim of this study is to establish a morphological model which can hindcast the Ley Bay evolution with high spatial and temporal resolution in order to observe the impacts of the *Leyhörn* peninsula in detail. Such a model provides more insight into the potential physical impacts and the governing morphological processes due to the peninsula construction.

Numerical models have become very popular in recent years to investigate the long-term morphological evolution. A well-established numerical model might be able to satisfactorily hindcast/forecast the morphological changes with high spatial and temporal resolution. Therefore, a numerical approach provides better insight on dominant processes of a system by consuming less amount of the measured data compared to the other data driven approaches (Elias, 2006; Homeier et al., 2010; Knaack and Niemeyer, 2001). Historical data in the Ley Bay area are very sparse and thus it is further encouraged to adopt a numerical model to investigate the formation and migration of the

* Corresponding author. Tel.: +49 1792 295540; fax: +49 1792 295676.
E-mail addresses: P.K.Dissanayake@swansea.ac.uk (P. Dissanayake), Andreas.Wurpts@nlwkn-ny.niedersachsen.de (A. Wurpts).
[1] Presently: Coastal and Estuary Group, College of Engineering, Swansea University, SA2 8PP, Swansea, UK.
[2] Tel.: +49 49 32 916 121; fax: +49 49 32 1394.

0378-3839/$ – see front matter.
http://dx.doi.org/10.1016/j.coastaleng.2013.08.005

morphological features by means of discrete modelling of the underlying processes.

The state-of-the-art Delft3D model is nowadays increasingly employed to analyse the long-term morphological evolution in the coastal and estuarine systems (e.g. Dastgheib et al., 2008; Dissanayake et al., 2009, 2012a, 2012b; Van der Wegen, 2010). These studies have shown that the tide dominated coastal systems can to a reasonable extent be modelled imposing the tidal boundary forcing only. Dissanayake et al. (2012b) discussed the limitations of the predicted Ley Bay morphology due to applying tidal forcings only and emphasised the requirement to include the wave boundary also for a better representation of the morphological features. Wave driven currents govern the littoral drift at the inlet/basin systems (i.e. enhancing flood transport and attenuating ebb transport). Inside the basin, wave–current interaction results in increased sediment mobility and that could lead to the enhancement of the sediment distribution in the Ley Bay as opposed to the predictions of Dissanayake et al. (2012b). Application of a wave climate to observe the morphological changes is a non trivial task because it is not effective to undertake brute-force long-term simulations and therefore wave schematisation is a prerequisite. The present study sufficiently overcomes this issue and simulates the Ley Bay morphology from 1975 to 1990 enforcing both tidal and wave boundaries into the Delft3D model under three sediment transport formulations. Resulting evolutions are analysed in terms of visual, statistical and quantitative methods in order to compare and contrast the anthropogenic effect on the Ley Bay morphology.

2. Study area

Ley Bay is a part of the Oster-Ems basin which is located between Borkum (west) and Juist (east) barrier islands in the East Frisian Wadden Sea (Fig. 1). The average tidal range of the Oster-Ems inlet is about 2.8 m and the yearly mean wave height seaward from the inlet is about 1 m. This inlet/basin system can be classified as a mixed-energy tide dominated environment (Hayes, 1979). Ley Bay is characterised by a hierarchy of tidal gullies and tributaries of the tidal inlet (Leysander Priel, Greetsieler Wattfahrwasser and Norder Außentief, see Fig. 1). A large part of the basin area consists of intertidal flats and extended supratidal salt marshes with unique fauna and flora. Human intervention in this area was demanded to mitigate the coastal zone management problems, i.e. safety against storms, navigational access of fishing vessels to Greetsiel harbour and maintaining inland drainage.

The catastrophic storm surges of the 14th century widened and extended the Ley Bay area. The flooded areas were highly vulnerable to erosion during storm surges, because the subsurface consisted of peat layers. After such events, the balance between tidal forcing and morphology was disturbed and strong sedimentation occurred to re-establish the dynamic equilibrium (Niemeyer, 1991). Then, salt marshes were developed at the borders of the bay which in turn enhanced the bay sedimentation together with the associated land reclamation work (Homeier, 1969). Growth of salt marshes allowed subsequent reclamation and diking of the formerly lost areas. In recent years, diking of inter-tidal flats rather than supratidal salt marsh areas has been implemented, which has a much higher impact on hydrodynamical–morphological interactions (Niemeyer, 1991). These measures ultimately resulted in accelerated sedimentation at the borders of the bay and in the access channel affecting the inland drainage and the navigational access respectively. Therefore, the inland drainage was performed by pumping water from the hinterland to the Ley Bay while the depth of the navigational channel was maintained in terms of dredging spending millions of Euros annually.

Several strategies were formulated in order to address these coastal management issues, of which the plan for enclosing of the Ley Bay area became more urgent because the existing dikes could not meet the

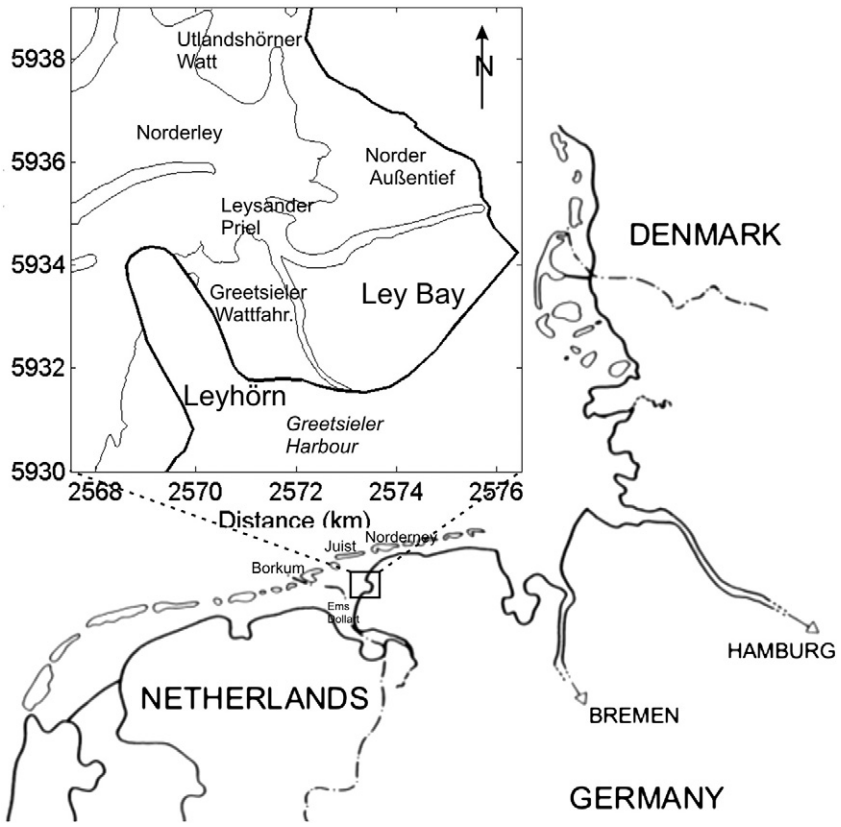

Fig. 1. Location of the Ley Bay area in the East Frisian Wadden Sea and its channel pattern.

safety requirements (Niemeyer, 1984). However, this option resulted in a controversial public discussion with respect to the economic and ecological implications (Hartung, 1983). Therefore, the State Government of Lower Saxony demanded another solution based on the newly established social priorities and the traditional coastal zone management strategies in the Wadden Sea area. As an alternative, the *Leyhörn* peninsula was constructed in 1984 to enable the following functionalities (Niemeyer, 1994),

- Safety of the coastal area against storm surges.
- Conservation of the Ley Bay as a unique ecological area.
- Re-establishment of inland drainage mainly by free-flow due to hydraulic gradients.
- Navigational access without maintenance dredging.
- Conservation of the traditional activities of the adjacent fishing harbour (i.e. Greetsiel, see Fig. 1).

3. Approach

3.1. Numerical modelling

Process-based model Delft3D is used to investigate the Ley Bay evolution. It allows one- (1D), two- (2DV and 2DH) and three-dimensional (3D) simulations. Discretisation of the study area can be in rectilinear, curvilinear or spherical co-ordinate systems. The primary variables of flow, water level and velocity, are specified on Arakawa C staggered grids. As 3D processes (e.g. cross-shore wave-induced currents, strong variations in the vertical flow structure (density stratification)) are not of critical importance to reach the objectives of the present study, here the depth-averaged version (2DH) of Delft3D is employed. Furthermore, previous studies (Dastgheib et al., 2008; Dissanayake et al., 2009, 2012a, 2012b; Van der Wegen and Roelvink, 2008; Van der Wegen et al., 2008) have shown that application of the 2DH version is able to reproduce major channel/shoal patterns of the Wadden Sea basins.

The model solves the unsteady shallow water equations via the alternating direction implicit (ADI) method to compute the hydrodynamics (Leendertse, 1987; Stelling, 1984; Stelling and Leendertse, 1991). The system of equations consists of the horizontal momentum equations, the continuity equation, the transport equation and a turbulence closure model. Wave driven currents are implemented into the model by imposing the depth-integrated wave forces in the momentum equations. The implementation of these equations in Delft3D is described in detail by Lesser et al. (2004) and is hence not reproduced here.

3.1.1. Sediment transport

Wave effects on the sediment transport in 2DH (due to breaking) are included in terms of wave-induced mass flux and increased bed shear stress. Other important wave effects such as streaming in the wave boundary layer are modelled as a time averaged shear stress. Dissanayake et al. (2012b) used both non-cohesive and cohesive sediment fractions to hindcast the Ley Bay evolution. A similar strategy is applied to estimate sediment transport in the present analysis too. Cohesive transport (≤0.063 mm) is computed using the Partheniades' erosion and Krone's deposition formulas (Partheniades, 1965). The maximum bed shear stress due to current and waves in this formula is defined based on the wave–current interaction implemented in the model. In contrast to the previous study, non-cohesive transport (>0.063 mm) is computed using three formulas, 1) Van Rijn (1993), 2) Soulsby (1997) and 3) Van Rijn et al. (2004), to investigate the sensitivity on the Ley Bay evolution.

3.1.1.1. Van Rijn 1993 formula (VR93). In Van Rijn's (1993) formulation, the sediment transport below and above the reference height '*a*' is defined as bed load and suspended load respectively. The '*a*' is mainly a function of water depth, a user defined reference factor and wave-induced ripple height. Sediment entrainment into the water column is facilitated by imposing a reference concentration at '*a*'.

$$a = \min\left[\max\left\{Fac.k_s, \frac{\Delta_r}{2}, 0.01h\right\}, 0.20h\right], \tag{1}$$

where a is Van Rijn's reference height (m); Fac is a user defined proportionality factor (−); k_s is a user-defined effective bed roughness height (m); Δ_r is a wave induced ripple height (0.025 m); and h is water depth (m).

Sediment mixing is separately estimated using current-related and wave-related vertical turbulent mixing coefficients as given in Van Rijn (1993). Suspended sediment transport is estimated based on the advection–diffusion equation. In depth-averaged simulations, the 3D advection–diffusion equation is approximated by the depth-integrated advection–diffusion equation:

$$\frac{\partial h\bar{c}}{\partial t} + \bar{u}\frac{\partial h\bar{c}}{\partial x} + \bar{v}\frac{\partial h\bar{c}}{\partial y} - D_H\frac{\partial^2 h\bar{c}}{\partial x^2} - D_H\frac{\partial^2 h\bar{c}}{\partial y^2} = h\frac{\bar{c}_{eq} - \bar{c}}{T_s}, \tag{2}$$

where D_H is the horizontal dispersion coefficient (m^2/s); $\bar{c}$ is the depth averaged sediment concentration (kg/m^3); $\bar{c}_{eq}$ is the depth-averaged equilibrium concentration (kg/m^3) as described by Van Rijn (1993) and T_s is an adaptation time-scale (s). T_s is given by (Galappatti, 1983),

$$T_s = \frac{h}{w}T_{sd}, \tag{3}$$

where, h is the water depth, w is the sediment fall velocity and T_{sd} is an analytical function of shear velocity u_* and w. Where, u_* is given by:

$$u'_{*,c} = \left(0.125 f'_c\right)^{0.5}\bar{u}. \tag{4}$$

Bed load sediment transport is estimated by:

$$|S_b| = f_{bed}\eta \times 0.5\rho_s d_{50} u'_* D_*^{-0.3} T_a, \tag{5}$$

where, D_* is a non-dimensional particle diameter,

$$D_* = d_{50}\left[\frac{(s-1)g}{\upsilon^2}\right]^{1/3}, \tag{6}$$

and, T_a is the non-dimensional bed shear stress,

$$T_a = \frac{\left(\tau'_b - \tau_{b,cr}\right)}{\tau_{b,cr}}. \tag{7}$$

For Eqs. (1)–(6), S_b, is the bed load transport rate (kg/m/s); f_{bed} is a calibration factor (−); η is the relative availability of sand at the bottom (−); d_{50} is the mean grain diameter (m); ρ_s is the density of sediment (kg/m^3); f'_c is the current-related friction factor (−); $\bar{u}$ is the depth average velocity (m/s); s is the relative sediment density (−); υ is the horizontal eddy viscosity (m^2/s); and, $\tau_{b,cr}$ is the critical bed shear stress for initiation of sediment transport (N/m^2). Bed shear stress (τ') is due to current (τ_c) and waves (τ_w): $\tau = \tau_c + \tau_w$.

3.1.1.2. Soulsby–Van Rijn formula (SVR). Soulsby (1997) proposed the following equation for the total sediment transport rate under current and waves:

$$q_t = A_s U\left[\left(U^2 + 0.018\frac{U_{rms}^2}{C_d}\right)^{0.5} - U_{cr}\right]^{2.4}(1 - 1.6\tan\beta), \tag{8}$$

where, q_t is the total sediment transport (kg/m/s); U is the depth averaged velocity (m/s); U_{rms} is the root-mean-squared wave orbital

velocity (m/s); C_d is the drag coefficient due to a current along (−); U_{cr} is the critical bed shear velocity (m/s); and β is the local bottom slope (−).

$A_s = A_{sb} + A_{ss}$, coefficients A_{sb} and A_{ss} are related to the bed load and the suspended load respectively and are given by,

$$A_{sb} = \frac{0.005h(d_{50}/h)^{1.2}}{[(s-1)gd_{50}]^{1.2}}, \quad (9)$$

$$A_{ss} = \frac{0.012d_{50}D_*^{-0.6}}{[(s-1)gd_{50}]^{1.2}}. \quad (10)$$

The current related drag coefficient is given by,

$$C_d = \left[\frac{0.4}{\ln(h/z_0)-1}\right]^2, \quad (11)$$

where, z_0 is equal to 0.006.

3.1.1.3. Van Rijn 2004 formula (VR04). In comparison to the Van Rijn (1993) formula, several features have been improved and implemented in the Van Rijn et al. (2004) sediment transport formula. Some of them are predictors of bed roughness (i.e. small-scale ripples, mega ripples and dune environments), predictor of suspended sediment size, grain roughness, friction factor and shields criterion for fine sand. Detailed description of this implementation is referred to Van Rijn et al. (2004).

Updated reference height reads as,

$$a = \max\left(0.5k_{s,c,r}, 0.5k_{s,w,r}, 0.01\right), \quad (12)$$

where, a is Van Rijn's reference height (m); $k_{s,c,r}$, is the current-related bed roughness height due to small-scale ripples (m); and $k_{s,w,r}$ is the wave-related bed roughness height due to small-scale ripples.

Table 1 indicates four major differences of these three formulas. Therefore, different sediment transport fluxes are expected in each case leading to different morphological changes.

3.1.2. Morphodynamics

Morphodynamic changes of coastal areas occur at larger time scales compared to the hydrodynamic time scales (Stive et al., 1990). The morphological scale factor (*MF*) approach presented by Roelvink (2006) and Lesser et al. (2004), which is used in Delft3D for bed level updates, is able to adequately bridge these two time scales. In this approach, which is particularly geared at significantly improving the efficiency of morphodynamic calculations, the bed level changes calculated at each hydrodynamic time step are scaled up by multiplying erosion and deposition fluxes by a constant (*MF*):

$$\Delta t_{\text{morphology}} = MF \times \Delta t_{hydrodynamic}. \quad (13)$$

This approach also allows accelerated bed level changes to be dynamically coupled (on-line) with hydrodynamic computations. In general usage, several trial simulations are undertaken with incremental *MF*s to determine the highest *MF* value that can be used safely for a given simulation. Sensitivity analysis of *MF* to hindcast the Ley Bay evolution is referred to Dissanayake et al. (2012b).

Table 1
Major differences of Van Rijn, 1993 (*VR93*), Soulsby–Van Rijn (*SVR*) and Van Rijn et al., 2004 (*VR04*) formulas.

Criterion	VR93	SVR	VR04
Bed roughness	User defined	User defined	Roughness predictor
Type of transport	Bed load Suspended load	Total load	Bed load Suspended load
Definition of bed/ suspended load	Reference height '*a*'	–	Modified 'a' with bed roughness predictor
Entrainment of sediment from bed	Reference concentration at 'a'	Skin-friction shear stress	Reference concentration at 'a'

3.2. Model implementation

3.2.1. Bathymetry and grid set-up

The model area covers the entire Oster-Ems basin. Fig. 2 shows the measured bathymetries (i.e. 1975 and 1990) and the grid set-up. It is emphasised that there is no bathymetry data available to represent the year of the peninsula construction (1984) and therefore it is substituted by implementing the 1990 peninsula configuration on the model predicted 1984 bed in this analysis. The 1975 morphology is taken as the initial model bed. The enclosed rectangle in Fig. 2b (1990 bed) indicates the Ley Bay area and the *Leyhörn* peninsula (see outline of the peninsula on the 1975 bed (Fig. 2a)). The averaged depth of the Ley Bay area (on the 1975 bed) is about +0.5 m MSL implying that tidal flats and salt marshes extend to a large part of the bay area. On the 1975 bathymetry, there is a well-pronounced channel system in the Ley Bay (see numbers 2, 3 and 4 in Fig. 2a). Leysander Priel (2 in Fig. 2a) is branched into two channels, namely Greetsieler Wattfahrwasser (3 in Fig. 2a) and Norder Außentief (4 in Fig. 2a). The Greetsieler channel provided the navigational access to the Greetsieler harbour while the Norder channel was mainly used for the inland drainage by pumping. On the 1990 bathymetry, the *Leyhörn* peninsula (length ~ 3.5 km and width ~ 1.5 km) is shown whereas the access channel is not yet found because it has been implemented in 1991 (Knaack and Niemeyer, 2001). The Ley Bay area shows strong sedimentation and the disappearance of the Greetsieler and Norder channels (Fig. 2b). However, Leysander Priel appears to have been more pronounced in comparison to the 1975 bathymetry. This is an indication of strong current pattern at the entrance of the bay due to the presence of the peninsula.

Fig. 2c shows the model grid enclosing the Oster-Ems basin. Averaged grid size is about 200 m × 200 m. However, the Ley Bay area (~5.0 km × 5.0 km) has a high resolution (20 m × 20 m) in order to represent the bay channel pattern.

3.2.2. Boundary forcing

Dissanayake et al. (2012b) discussed the Ley Bay evolution under tidal forcings only. Predicted morphological features indicated that the sediment distribution in the bay has been underestimated. Waves stir sediment from the bottom and that is expected to increase the distribution inside the bay. As such, present analysis uses both tidal and wave boundary forcings.

3.2.2.1. Tidal boundary. Tidal forcing of the Oster-Ems model is based on the Continental shelf model which is well calibrated and enclosed the entire North Sea area (Verboom et al., 1992). The offshore (North Sea) tide was transformed up to the model boundaries (Wadden Sea) by a nested modelling approach. Model nesting consisted of two phases, 1) continental shelf model to coastal model, and 2) coastal model to Oster-Ems model. Initially, the continental shelf model was simulated for 3 months from June to September in 1975 based on the astronomical boundary conditions and then the water level elevations were extracted at the boundaries of the coastal model. Subsequently, the coastal model (see Knaack et al., 2003) was simulated using the extracted water levels to get the boundary forcings of the Oster-Ems model which has three open boundaries viz. north, east and west. The north boundary is located at the inlet gorge and the east and west boundaries are in the Wadden Sea side opposite the Norderney tidal basin and the Ems estuary respectively (see Fig. 1). Preliminary results showed that applying three water level boundaries of the Oster-Ems model (at north, east and west), developed unrealistic velocity patterns. Therefore, flow velocity is applied for the northern boundary while the lateral two boundaries

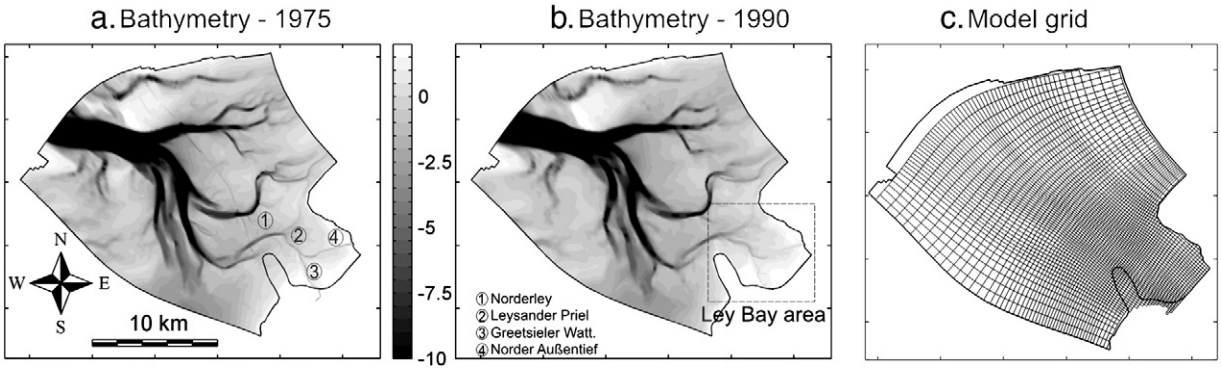

Fig. 2. Measured bathymetries of the model area (Oster-Ems basin), 1975 bed with the layout of *Leyhörn* (a), 1990 bed with the Ley Bay analysis area (b) and Model grid (every 5th grid line shown) (c).

(i.e. east and west) use water levels. Such a combination of boundary forcings increases the numerical stability (see Delft3D user manual).

3.2.2.2. Wave boundary. Wave boundary of this analysis is based on the HIPOCAS data set (Herman et al., 2007) at a location about 20 m deep in front of the Norderney island (i.e. adjacent island to the east of Juist). The data set consists of H_s (m), T_p (s) and direction (nautical) with the wind speed (m/s) and direction (nautical) in 30 minute intervals. Present analysis spans from 1975 to 1990 and therefore the HIPOCAS data of the respective period are used to define the wave boundary. Fig. 3 shows the wave and wind roses in the modelling period.

It is inevitable to apply a highly schematised wave climate in a morphological simulation due to the unaffordable computational time (see Dissanayake, 2011). The present wave climate is schematised employing two filtering techniques. First is based on the probability of occurrence and the second considers the relative contribution of each wave condition to the overall bed level change.

3.2.2.2.1. Probability of occurrence. Selected time series of waves and winds from 1975 to 1990 were initially formulated into the scatter diagrams with wave height and directional classes. Wave height classes have 1 m intervals while the directional classes have 20 degree intervals. In case of waves, there are four scatter diagrams representing probability of occurrence, *Hs*, *Tp* and direction. Wind parameters consist of two scatter diagrams for the wind speed and direction in the same wave height and directional classes. A scatter diagram with the probability of occurrence indicates the probability of each wave cluster in the respective height and directional classes. Each probability has corresponding wave and wind parameters. In order to simplify the analysis, it was assumed that wave conditions with a probability of occurrence less than 0.01% rarely occurs. Further, it is expected that strong morphological changes due to the extreme events (i.e. low probability cases) are reshaped by the calm periods. Therefore, the wave conditions which have a probability lower than 0.01% were discarded from the analysis (see probabilities with bold numbers, Table 2). In this case, 14 events which consist of a total probability of 0.06 were removed from the analysis. This implies that the probability of occurrence of the entire wave climate decreases from 100 to 99.94. There are 73 events left according to the remaining probability clusters. It is still required to reduce the number of events in order to apply the morphological simulation.

3.2.2.2.2. Relative contribution of each wave condition to the bed level changes. The selected 73 wave conditions are further schematised based on their contributions to the overall bed level change of the wave climate. Short-term simulations (i.e. 2 days) were carried out applying each wave condition separately and then the analysis used the resulting 73 sedimentation and erosion patterns. This is an iterative approach (i.e. *OPTI* routine, per. com. with Dano Roelvink) which determines the overall bed level change of the wave climate and the relative contribution of each wave condition to the overall change. First, the overall bed level change of the wave climate is estimated by linear summation of these 73 sedimentation and erosion patterns after multiplying with their corresponding probability of occurrence. Then at each iteration step, the contribution of each wave condition to the overall change is assessed in terms of statistical parameters (i.e. *RMS* error, R^2, *standard deviation*, *bias*, *covariant* etc.). Next the wave condition which has the lowest contribution (e.g. highest R^2) is thrown away. The relative contribution of the remaining wave conditions is given by weight factors for all remaining conditions. This iteration procedure continues

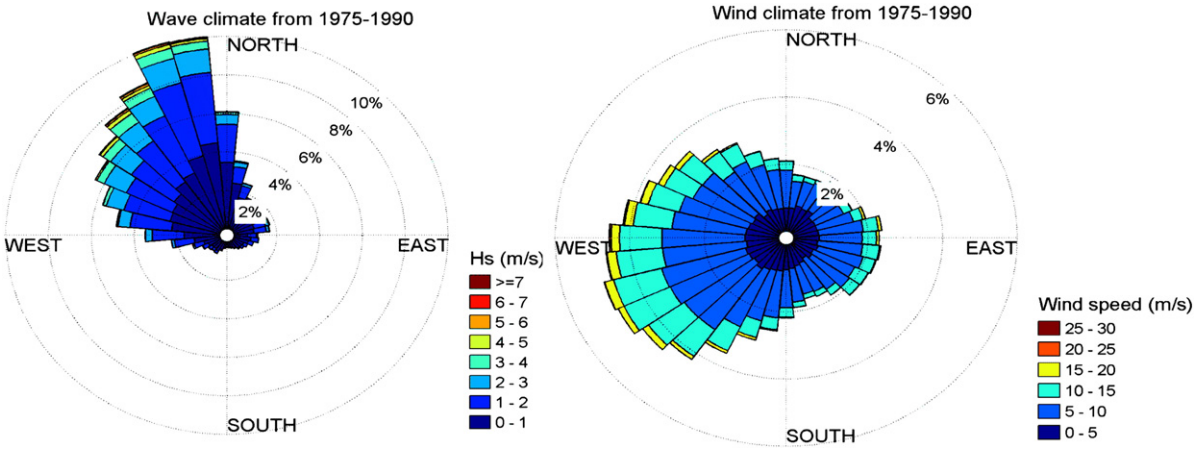

Fig. 3. Wave (a) and Wind (b) roses for the period 1975 to 1990 based on the HIPOCAS data set (Herman et al., 2007).

Table 2
Scatter diagram indicating probability of occurrence for the defined wave height and directional classes.

Hs(m) \ Directional classes (deg. Nau.)	0–20	20–40	40–60	60–80	80–100	100–120	120–140	140–160	160–180	180–200	200–220	220–240	240–260	260–280	280–300	300–320	320–340	340–360	Prob.
0–1	4.8946	2.6373	1.9557	1.9422	1.4623	1.3896	1.0374	0.7814	0.5682	0.6196	1.0616	1.0623	1.6648	3.4088	4.8062	5.4393	6.5331	8.5052	**49.77**
1–2	1.9329	0.9347	0.9711	1.1187	0.9233	0.4962	0.2745	0.1055	0.0848	0.0984	0.2567	0.3929	1.0153	2.9425	4.5346	4.8055	6.5274	6.9951	**34.41**
2–3	0.4969	0.1462	0.2061	0.3087	0.1112	0.0135	**0.0007**	**0.0021**	**0.0014**	**0.0036**	0.0193	0.0356	0.1476	0.6431	1.7133	2.4063	2.2495	2.2844	**10.79**
3–4	0.0977	0.0314	0.0235	0.0513	**0.0029**	–	–	–	–	–	–	–	0.0121	0.0563	0.3529	0.9440	1.0032	0.7829	**3.36**
4–5	0.0399	–	**0.0050**	**0.0100**	–	–	–	–	–	–	–	–	**0.0014**	**0.0014**	0.0592	0.3237	0.3429	0.2716	**1.06**
5–6	**0.0071**	–	–	**0.0064**	–	–	–	–	–	–	–	–	–	–	**0.0086**	0.0863	0.2182	0.0984	**0.42**
6–7	–	–	–	–	–	–	–	–	–	–	–	–	–	–	–	0.0321	0.0834	0.0321	**0.15**
7–8	–	–	–	–	–	–	–	–	–	–	–	–	–	–	–	**0.0014**	0.0250	0.0150	**0.04**
8–9	–	–	–	–	–	–	–	–	–	–	–	–	–	–	–	–	–	**0.0036**	**0.00**
Prob.	**7.47**	**3.75**	**3.16**	**3.44**	**2.50**	**1.90**	**1.31**	**0.89**	**0.65**	**0.72**	**1.34**	**1.49**	**2.84**	**7.05**	**11.47**	**14.04**	**16.98**	**18.99**	**100**

until one wave condition remains. Resulting statistical parameters indicate how well the overall bed level change agrees with that of the reduced number of conditions. Further, weight factors show the relative contribution of remaining waves at each iteration step. By analysing the variation of statistical parameters, a few wave conditions can be selected based on the point at which first indicates a significant change in gradient compared to the previous iteration steps.

Fig. 4 shows variation of the *RMS* error and R^2 in the present analysis considering the erosion/sedimentation patterns in the Ley Bay. Applying all 73 conditions, the *RMS* is equal to zero and R^2 is 1. The value of these parameters increases and decreases respectively while one wave condition is leaving at each iteration step. A significant change between consecutive iteration steps begins from the last 4 to 3 conditions in both parameters. These observations comply with the other statistical parameters as well (i.e. *bias*, *covariant*, etc.) Therefore, the predicted sedimentation/erosion pattern of all wave conditions (73), 4 wave conditions and 1 wave condition are further qualitatively compared and contrasted together.

Resulting sedimentation/erosion patterns of the Ley Bay area are shown in Fig. 5 for the above three cases (red — Sedimentation, blue — Erosion). A qualitative comparison between all 73 and the selected 4 conditions indicates that they are almost similar while the case considering only a single condition differs.

According to the schematization approach, the last 4 wave conditions sufficiently reproduce the bed level change of the wave climate. The overall objective of this study is to hindcast the bed level change of the Ley Bay area. Therefore, applying the selected wave conditions which are based on the bed level change, is expected to result in the Ley Bay evolution as in case of the wave climate.

Table 3 shows the selected four wave conditions and their weight factors together with the corresponding wind speed and direction. The wind characteristics are obtained from the wind speed and direction scatter diagrams by referring to the respective wave height and directional classes of the probability of occurrence. As mentioned earlier, the weight factors indicate the relative contribution of each wave condition to the overall bed level change. The highest weight factor is related to the lowest wave height which comes from the east. Lower weight factors are attributed to the higher wave heights in the west–northwest (WNW) sector . Therefore, the weight factor does not necessarily represent the dominant direction (i.e. WNW) of the wave climate. In fact, they indicate that the strong bed level changes of higher wave heights are reshaped by calm periods (i.e. small wave heights).

3.2.3. Selection of MORFAC

The Delft3D model uses the *MF* technique to simulate long-term bed evolutions (see Section 3.1.2). Dissanayake et al. (2012b) showed the sensitivity of the Ley Bay evolution to the *MF* value (i.e. applying incremental values of 30, 60 and 120) under tidal boundary forcings only. The optimum value of this study is 60. Under both tidal and wave boundary forcings, it is expected that the rate of sediment transport increases compared to that of the tidal forcings only and so does the bed level change. Therefore, the *MF* value of the present study should necessarily be less than 60.

Sediment transport fluxes change based on the wave condition and therefore application of *MF* must be correlated to the respective weight factor. Single and multiple *MF* approaches are used to implement *MF* with different wave conditions (Dastgheib, 2012; Dissanayake, 2011). In the case of multiple *MF*s, each wave condition has a unique *MF* value and they are applied using a single hydrodynamic period. It is noted that applying multiple *MF* values might give rise to mass balance error based on the tidal phase at which the *MF* is changed to another value (Dissanayake, 2011). In order to avoid this difficulty, the present analysis adopts the single *MF* approach in which one *MF* value is used for all wave conditions considering different hydrodynamic periods with respect to their weight factors.

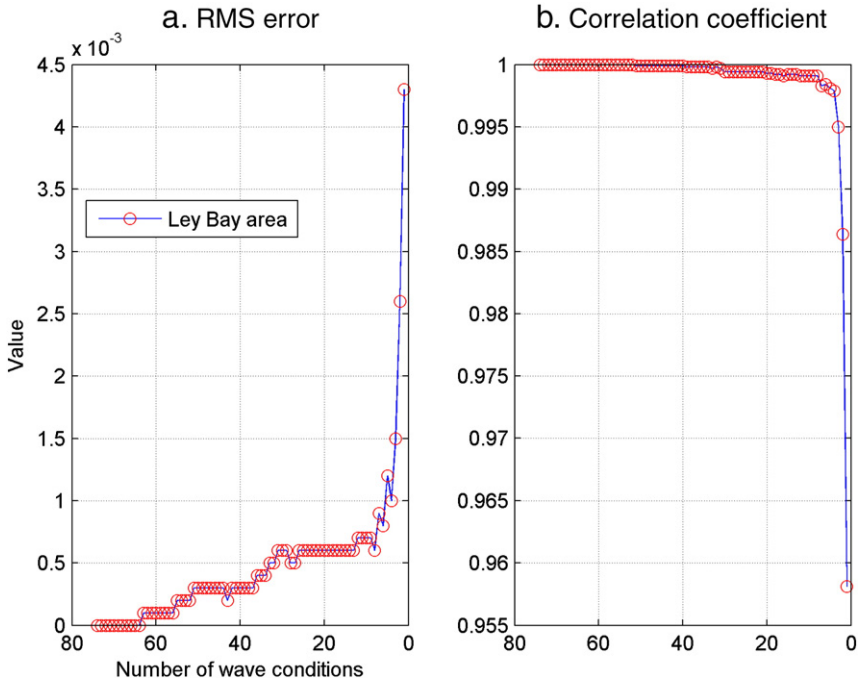

Fig. 4. Variation of *RMS* error (a) and R^2 (b) after deducting one wave condition at each iteration step.

In this analysis, wave conditions are applied in order to produce increased repetitions of each condition (i.e. lower duration and higher occurrence) with a single *MF*. Such an approach is expected to be more realistic rather than applying four hydrodynamic durations (i.e. for 4 waves) of the simulation period. The implementation uses a predefined hydrodynamic period ($T_{hyd} = 35$ days) consisting of two spring-neap tidal cycles in such a way that it can accommodate all 4 wave conditions in respect of their weight factors. This hydrodynamic period is again classified into sub-hydrodynamic units of 5 days (t_{sub}) to apply increased wave repetitions. They indicate spring-tide, neap-tide and intermediate-tide (i.e. tidal period in between spring and neap or neap and spring) periods of T_{hyd}. The smallest hydrodynamic duration of a wave condition (t_{wave}) is taken as 12 h such that t_{sub} allows one to apply all four wave conditions proportional to their weight factors (see Table 4).

According to the selected values, the t_{sub} repeats 7 times (i.e. 35/5) in T_{hyd} and thus generates increased repetitions of wave conditions (i.e. each wave repeats 7 times during the simulation) in contrast to the implementation of Dissanayake (2011). Furthermore, the T_{hyd} can be repeated in order to get the *MF* value as lower as required. Final definition of the *MF* follows as,

$$MF = \frac{T_{mor}}{\left[(n_1 + n_2 + n_3 + n_4) \times t_{wave} \times \frac{T_{hyd}}{t_{sub}} \times N\right]}, \quad (14)$$

where, n is the number of t_{wave} corresponding to the weight factor of each wave W_1, W_2, W_3 and W_4; N is the number of repetitions and T_{mor} is the morphological period

Application of the above values resulted in the *MF* value of 45.35. This is computationally efficient (i.e. lower *MF* value demands longer simulation period) and consistent with that of the MF_{tide} (i.e. decrease by about 25% compared to the tidal boundary only, $MF_{\text{tide}} = 60$) and therefore was employed in the morphological simulation hereafter.

3.2.4. Bed sediment composition

Dissanayake et al. (2012b) investigated the Ley Bay evolution applying different combination of sediment fractions. Results showed the

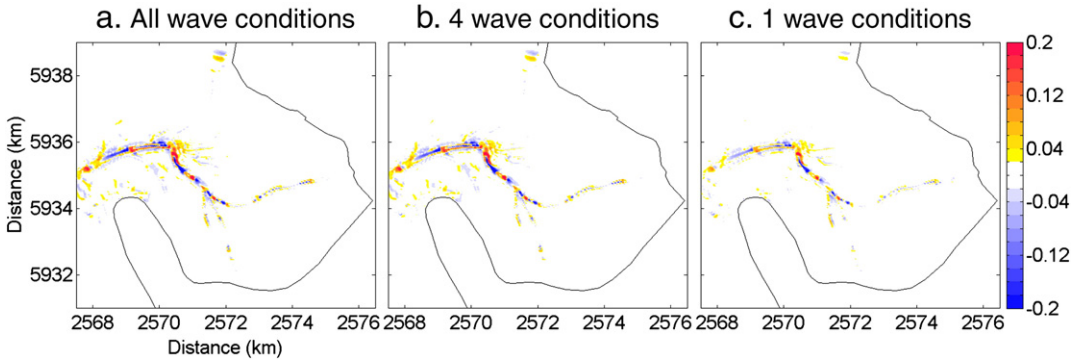

Fig. 5. Predicted sedimentation/erosion pattern of all (73) wave conditions (a), 4 wave conditions (b) and 1 wave condition (c).

Table 3
Schematised four wave conditions to hindcast the Ley Bay evolution.

Wave no.	Hs (m)	Tp (s)	Dir (deg. Nau.)	Weight factor	Wind speed (m/s)	Wind dir. (deg. Nau.)
W1	0.6	3.9	90	0.5	6.8	108
W2	1.4	5.3	271	0.3	10.2	219
W3	3.4	9.0	330	0.1	12.9	293
W4	1.4	6.8	331	0.1	6.9	270

Table 4
Wave conditions with their implementation in a 5 day period.

Wave no.	Weight factor	No. of t_{wave}
W1	0.5	5
W2	0.3	3
W3	0.1	1
W4	0.1	1

optimum bed evolution under the application of an initially distributed sediment fractions with mud (≤0.063 mm), fine-sand (0.25 mm) and coarse-sand (0.60 mm). Therefore, the present simulations also incorporated the same initial bed sediment composition (see Fig. 6).

The model bed has vertical and horizontal discretisations of sediment fractions. The bed stratigraphy consists of 10 layers vertically 1 m thick, of which the first six layers (from top to bottom) have spatially varying mixtures of mud, fine-sand and coarse-sand (i.e. resulting layers of initial sediment distribution model, see Dissanayake et al., 2012b). The last four layers consist of a uniform mixture of fine-sand and coarse-sand (i.e. 50% of each fraction based on sediment mass).

This initial bed sediment composition is implemented into the model using layered bed stratigraphy (refer to Delft3D FLOW user manual). At the first time step, the topmost layer is divided into the transport layer (0.4 m following Dissanayake et al., 2012b) and the first under layer. During erosion, sediment is lost from the transport layer and that is recharged by the first under layer. After the sediment content of the first under layer is empty, the second under layer contributes to the transport layer and so on. During sedimentation, the transport layer receives sediment and passes into a newly created layer underneath. After the new layer is saturated (i.e. 1 m thickness in our analysis), a new under layer is formed between the transport layer and the saturated layer and so on. The maximum number of new layers is based on a user defined value (i.e. 10 in this case). Bed topography decreases by shrinking under layers during erosion and increases by expanding them during sedimentation. Sensitivity analysis undertaken in this study showed that applying 10 m of under layers allows continuous erosion during the simulations without depleting the sediment source in the grid-cells.

Erosion of sand fractions from the sediment bed and in turn the transport capacity depends on the mud content at the bed surface due

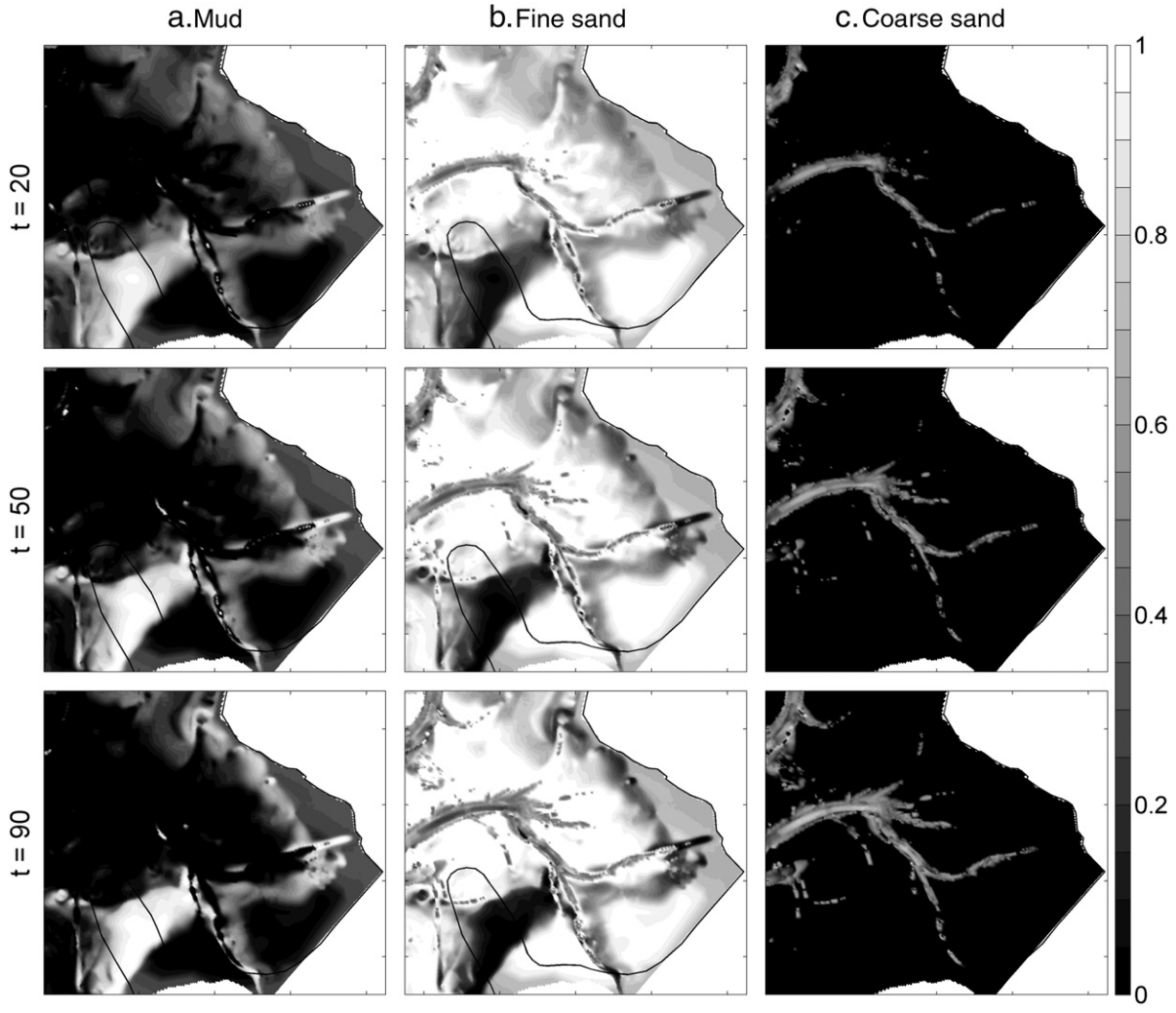

Fig. 6. Initially distributed bed sediment fractions of the top layer; a) Mud, b) Fine-sand and c) Coarse-sand after t = 20, 50 and 90 days (from Dissanayake et al., 2012b).

Table 5
Morphological simulations from 1975 to 1990 under two stages applying different transport formulas.

Sediment transport formula	Morphological Period (years)	
	Stage 1: 1975–1984	*Stage 2*: 1984–1990
Van Rijn (1993) (*VR93*)	9	6
Soulsby (1997) (*SVR*)	9	6
Van Rijn et al. (2004) (*VR04*)	9	6

to the fact that the fine particles easily escape to the water column compared to the coarse particles. However, deposition of sediment is assumed to be independent for sand and mud. Erosion of mud is determined by the user defined erosion parameter. Sensitivity of Ley Bay evolution to the mud-related parameters has been extensively discussed in Dissanayake et al. (2012b) and is referred therein.

At the open boundaries, no sediment concentration is prescribed for mud and sand fractions (i.e. initial concentration is 0) whereas suspended sediment, advected by tidal movement, is present. This means that sediment will leave the model domain and ideally come back after turning of the tide at the boundaries. This process is implemented in the model in terms of a *Thatcher–Harleman* time lag that stores sediment concentrations and reintroduces it at the boundary when the tide returns. However, this is probably more applicable for fine particles. Another option is adopted to consider the sand-sized particles in which at all inflow boundaries, flow enters carrying all sand sediment fractions at their equilibrium concentration profiles. Therefore, it can be expected that nearly perfectly adapted flow will enter to the domain.

3.2.5. Model simulations

Hydrodynamic behaviour of the model area was discussed in the previous study (Dissanayake et al., 2012b). The present study investigates the Ley Bay evolution applying both tidal and wave boundary forcings. The model bed consists of an initially distributed bed sediment composition (see Section 3.2.4). Sensitivity of bed evolution is analysed under three sediment transport formulas (see Table 5).

Morphological simulations span a period of 15 years from 1975 to 1990 in two stages, 1) *No-peninsula stage* and 2) *Peninsula stage*. The no-peninsula stage extends from 1975 to 1984 considering the fact that the peninsula was constructed in 1984. The predicted 1984 bed was subsequently used as the initial bed to simulate the second stage from 1984 to 1990. It is noted that the peninsula configuration was implemented on the 1984 predicted bed based on the 1990 data. Elevated bed topography was applied to represent the dyke around the peninsula while thin-dams (i.e. blocking the flow and so sediment transport through the grid-cell boundary without bed level change) characterise the training walls of the navigational access channel (see northern end of the peninsula in Fig. 7b). These simulations used the selected *MF* value of 45.35 (see Section 3.2.3).

Table 5 shows the morphological simulations in the present study.

It is emphasised that these models are simulated without including dredging and dumping work which have been undertaken:

- Prior to the peninsula construction.
  For maintenance of the navigational channel to the Greetsiel harbour (i.e. Greetsieler Wattfahrwasser) and for inland drainage (i.e. Greetsieler Wattfahrwasser and Norder Außentief) (see Fig. 1).
- During the peninsula construction.
  Construction of the outer dyke of the peninsula and deepening the enclosed area.

These activities are expected to have an impact on the Ley Bay morphology and thus predicted evolution could show some discrepancies in comparison to the measured data.

4. Results

The resulting bed evolutions were analysed under three comparisons; *Visual*, *Statistical* and *Quantitative*; in order to contrast the prediction under each formula and to find the best agreement with the data.

4.1. Visual comparison

4.1.1. Bed evolution

Fig. 7 shows the predicted 1990 morphologies under different transport formulas in comparison to the measured 1975 and 1990 data. The Ley Bay area is characterised by a pattern of very shallow channels and shoals including a large area of tidal flats (see depth ranges in Fig. 7a and b). On the 1975 bed, the outline shows the proposed peninsula, *Leyhörn*. On the 1990 bed, there is no navigational access channel through the peninsula because it has been implemented in 1991 (see Fig. 7b). A branch from the channel located at the NW corner of the model area has been developed on the 1990 bed increasing sediment supply into the bay. From 1975 to 1990, the measured data indicate strong sedimentation in the bay and the disappearance of the basin channel pattern (refer to depth contours in Fig. 7a and b). However, the main Ley Bay channel, Leysander Priel (see Fig. 1), appears to be more pronounced on the 1990 bed than on the 1975 bed. This is an indication of the accelerated velocity pattern at the entrance of the Ley Bay due to the presence of the peninsula.

Generally, the predicted channel pattern of the *VR93* is irregular compared to the results of the *SVR* and *VR04* (see at the Ley Bay entrance of Fig. 7b, c and d). In the case of *SVR* (d), there are no strong changes around the training walls (i.e. implemented in terms of the thin-dams, see Section 3.2.5). In contrast, the results of *VR93* (c) and *VR04* (e) indicate erosion to the west and accretion to the east of the training walls implying a strong contribution to the bed evolution rather than the latter case. All predictions show a growth of the eastward channel orientation in the bay and accretion in the southern channel as found on the measured 1990 bed. However, it appears that these two features

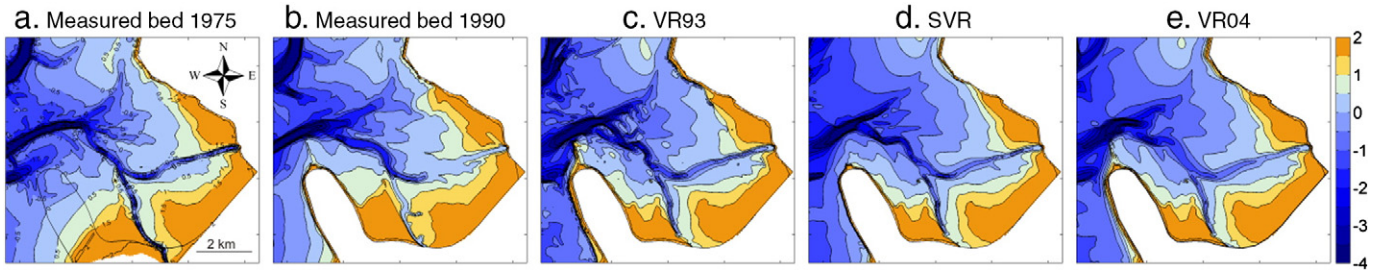

Fig. 7. Ley Bay morphology; measured beds, 1975 (a) and 1990 (b); predicted 1990 beds, Van Rijn, 1993 (c, *VR93*), Soulsby–Van Rijn (d, *SVR*) and Van Rijn et al., 2004 (e, *VR04*) (note. both *x* and *y* axes are in the same scale as given in Fig. 7a (i.e. 2 km scale bar) and also refer to the depth contours therein).

are better represented in the case of *VR04*. The predicted bed of the *VR04* further indicates a strong eastward channel at the entrance of the bay in comparison to the data. These are evidences of the different channel/shoal configurations of the Ley Bay based on the applied transport formula to compute the sediment transport in the model.

4.1.2. Sedimentation/erosion pattern

Fig. 8 shows sedimentation and erosion patterns of the data and the model predictions during the period from 1975 to 1990. In the data, strong sedimentation is found around the peninsula, in the middle of the bay and in the bay channels while the erosion areas are concentrated only along the channels. In fact, all model predictions have relatively larger erosion areas in comparison to the data and sedimentation along the channels and around the peninsula. Predicted sedimentation/erosion patterns along the bay channels tend to agree with the data. However, the channel at the northwest corner of the domain implies a different behaviour. Data indicate northward sedimentation and southward erosion while the models predict the opposite (compare *a* with *b*, *c*, *d*). Such a difference is probably attributed to the application of a highly schematised wave climate. It is emphasised that our main focus is on the Ley Bay evolution and therefore the wave schematization was based on the morphological evolution in the Ley Bay area only (see Fig. 5). No bed level change at the northwest corner of the domain was observed in the wave analysis. This could be due to the fact that the employed morphological period of the wave analysis is not long enough to develop bed level changes there. However, we restricted to such a period considering the sufficient bed level changes found in the Ley Bay and the required computational time (i.e. ~1 day for each wave run, see Section 3.2.2.2). Missing sedimentation areas in the middle of the bay are expected due to the human intervention on the bay morphology (i.e. dredging/dumping undertaken prior to the peninsula or during the construction period). These information are very scarce and hard to find and therefore were not included in these simulations. Similar phenomena could cause erosion areas to the west of the peninsula (i.e. sediment dumping is expected there during deepening inside the peninsula). According to the erosion/sedimentation patterns, the channel sedimentation in the bay appears to have been captured by *VR04* in comparison to the other two formulas.

4.1.3. Sediment transport on the 1990 predicted bed

Sediment transport patterns were estimated on the 1990 predicted bed applying the corresponding transport formula. Fig. 9 shows the total transport magnitude ($m^3/s/m$) of the three sediment fractions during the mid-flood condition (i.e. strong velocities and in turn strong sediment transport, see Dissanayake et al., 2009). All models indicate that the transport paths are concentrated only along the channels. The effect of transport formulas is found by their spatial extents. At the northwest of the model domain, *VR93* (Fig. 9a) shows a transport path to the north of the main channel while it appears to the south in the other two cases of which the *SVR* (b) has a strong pattern. At the entrance of the Ley Bay, each case shows different transport paths. The *VR93* has the largest extension of the transport along the southwest–northeast channel and also it consists of individual transport patches around the entrance compared to the other two cases. Both *VR93* and *SVR* show narrow transport paths while they are wider and stronger in the *VR04* (c). All models tend to produce eastward oriented transport in the Ley Bay and it is apparent in the case of *SVR*. These changes in transport patterns occurred due to two reasons, 1) difference of the initial bathymetry (i.e. predicted 1990 bed under each formula) and 2) application of different transport formulas.

4.2. Statistical comparison

In the statistical comparison, the enclosed area was limited to the Ley Bay only (see Fig. 2b) according to the main objective of the study. Two statistical parameters, correlation coefficient (R^2) and Brier skill score (*BSS*), were computed in order to determine the similarity of the measured bed and the predicted beds under different transport formulas.

4.2.1. Correlation coefficient

Bed level changes (not predicted bed levels) are used in the estimation of the R^2 to ensure that the areas of no change (note: a large part of Ley Bay (~60%) consists of supra-tidal and salt marshes) are not included in the calculation. This guarantees that there is no bias towards the high R^2 values due to the presence of such 'no change' areas inherent in the bathymetry (see further in Dissanayake, 2011). The R^2 is defined as,

$$R^2 = 1 - \frac{\sum (\Delta z_X - \Delta z_Y)^2}{\sum (\Delta z_X - \langle \Delta z_X \rangle)^2}. \tag{15}$$

It is noted that there is no 1984 measured data set. Therefore, the bed level change is always estimated with respect to the 1975 data. Δz_x is the bed level change between 1975 and 1990 measured data while Δz_y is the predicted relative bed level under different transport formulas with respect to the 1975 data. A higher R^2 value indicates higher similarity between model prediction and the data and vice versa.

Fig. 10 shows the variation of the R^2 value during the stage 2 simulation from 1984 to 1990. Under all cases, the predicted 1984 bed has a value of about 0.2. As mentioned earlier, there is no measured bed at 1984 in which the peninsula has been constructed. Therefore, the peninsula was implemented based on the 1990 bed configuration on the predicted 1984 bed in each case from the stage 1 simulation (from 1975 to 1984). Apparently, this gives rise to higher bed level changes compared to the model predicted evolution on the initial 1984 model bed. Thereafter, the R^2 values indicate the effect of different formulas on the bed evolution. Resulting evolution of the *VR04* has a relatively constant variation compared to the others and has the highest final value (~0.16) corresponding to the 1990 bed. Both *VR93* and *SVR* show a decreasing trend throughout the morphological period and the lowest value (~0.01) of the predicted 1990 bed is found under *VR93* while it is about 0.04 of *SVR*. The R^2 variation indicates that the predicted

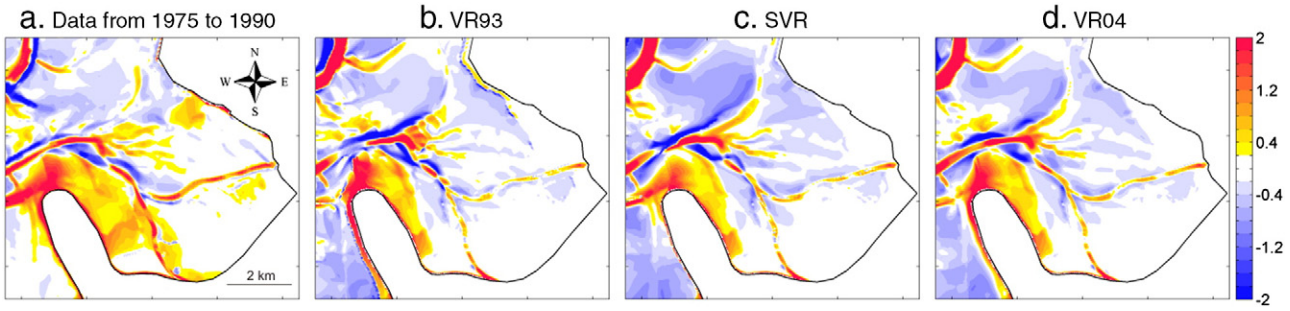

Fig. 8. Sedimentation/erosion pattern in the Ley Bay; data from 1975 to 1990 (a), Van Rijn, 1993 (b, *VR93*), Soulsby–Van Rijn (c, *SVR*), Van Rijn et al., 2004 (d, *VR04*).

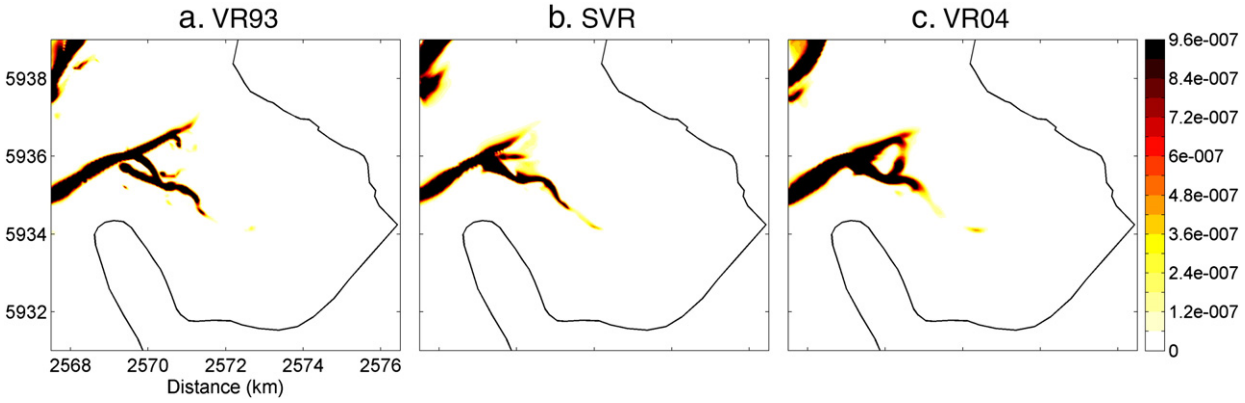

Fig. 9. Total sediment transport (m3/s/m) on the 1990 predicted bed under mid-flood condition; Van Rijn, 1993 (a, VR93), Soulsby–Van Rijn (b, SVR), Van Rijn et al., 2004 (c, VR04).

Ley Bay morphology of the *VR04* formula has a higher agreement with the data compared to the other two formulas.

4.2.2. Brier skill score

As has been discussed in Dissanayake et al. (2012b), the present analysis uses the *BSS* classification of Sutherland et al. (2004) in which the bed level changes are evaluated in terms of *phase*, *amplitude* and *mean value*. A perfect model prediction is expected to have 1, 0 and 0 corresponding to these three parameters leading to a value of 1 for the *BSS*. This analysis uses the measured 1975 bed (B), the measured 1990 bed (X) and the 1990 predictions under different formulas (Y).

Resulting *BSS* values and their parameters are given in Fig. 11 for all three cases with different transport formulas. Only the *VR04* case shows an increasing phase while it is decreasing in the other two. This means that the location of bed levels is better resembled with the data under *VR04* in comparison to the other formulas. Lowest amplitudes are also found with *VR04* during the evolution. From 1984 to 1988, both *VR93* and *SVR* indicate similar variation and thereafter *VR93* increases strongly up to about 0.15 while the other reaches about 0.1. Amplitude indicates magnitude of bed levels and the lower the value the better the agreement with the data. Only in the case of mean values, *VR04* shows a different behaviour compared to the previous two parameters. The *VR04* values vary between *SVR* and *VR93* values of which they have the highest and the lowest values respectively. The *BSS* shows a significant difference among the formulas. The *VR04* has relatively constant values and the final value is higher than 0.15. In contrast, both *VR93* and *SVR* have decreasing trends leading to a final value of about 0.05. Sutherland et al. (2004) have defined different classifications of the comparison based on the resulting *BSS* value (see Table 1 in Dissanayake et al. (2012b)). Accordingly, the *VR04* prediction qualifies as '*Reasonable/Fair*' while the other two are in the '*Poor*' category.

Statistical comparison (R^2, *BSS*) also indicated that the predicted Ley Bay morphology of the *VR04* formula better agrees with the data rather than that of the other two formulas. In order to further investigate these findings, evolution of the morphological elements in the Ley Bay is quantitatively analysed.

4.3. Quantitative comparison

Quantitative comparison was systematically undertaken to investigate the Ley Bay evolution in *Stage 2* under the three transport formulas. Initially, overall geometry was estimated by evaluating the basin hypsometry. Then, the resulting volume change was computed with respect to erosion and sedimentation volume. Finally, the evolution of individual elements were analysed in terms of channels and tidal flats in the Ley Bay.

4.3.1. Ley Bay hypsometry

Hypsometry indicates the relation of the basin wet surface area with the basin depth. Therefore, the higher the depth is, the lower the area

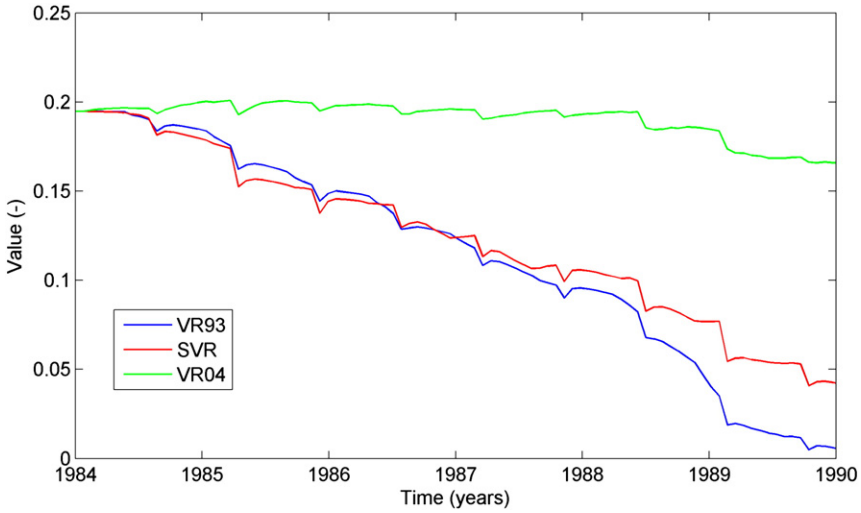

Fig. 10. Variation of R^2 value of the bed evolution under different transport formulas; Van Rijn, 1993 — blue-line (*VR93*), Soulsby–Van Rijn — red-line (*SVR*), Van Rijn et al., 2004 — green-line (*VR04*).

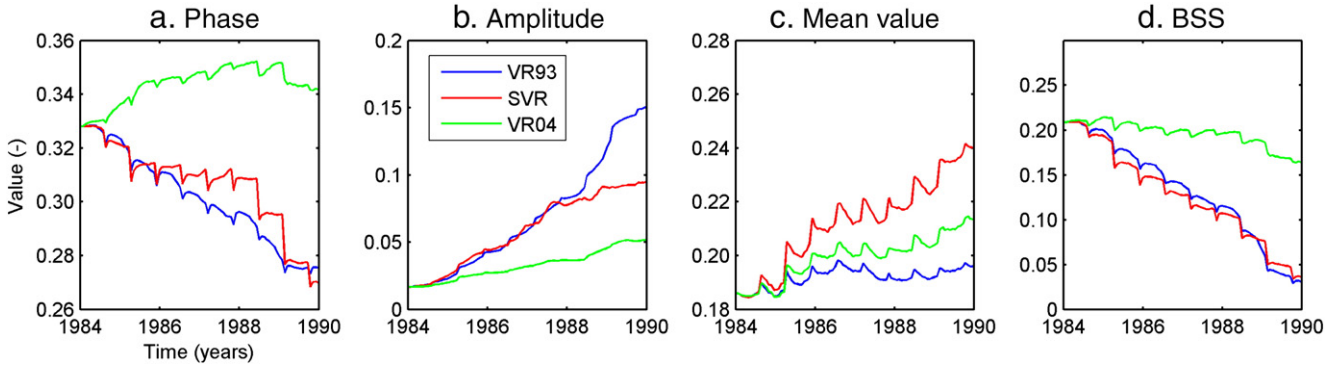

Fig. 11. Variation of *BSS* parameters of the bed evolution under different transport formulas; phase (a), amplitude (b), mean value (c) and *BSS* (d) in Van Rijn, 1993 — blue-line (*VR93*), Soulsby–Van Rijn — red-line (*SVR*), Van Rijn et al., 2004 — green-line (*VR04*).

and vice versa. Furthermore, decreasing the wet surface area during the evolution implies that sediment receives into the bay leading to decrease the channel area. Inverse applies for a sediment exporting system.

Fig. 12 shows the hypsometry curves for the measured data (1975 and 1990) and the predicted 1990 beds under the three formulas. The curve of the 1990 data is located to the left of that of the 1975 data (see dash-line and black-line). At MSL, the 1975 bed has an area of 6.74 km^2 while it is 6.21 km^2 for the 1990 bed. It is further evident that a large amount of sediment has been deposited around −0.5 m + MSL and +0.5 m + MSL. These are indications of sediment accumulation in the Ley Bay from 1975 to 1990. All models have predicted sedimentation at deep areas of the bay (i.e. depth > −3 m + MSL) and the strongest sedimentation is found under *VR04* (green-line). From −3 m + MSL to −1.5 m + MSL, the *VR04* shows marginal erosion compared to the other two cases. From −1.5 m + MSL to −0.5 m + MSL, all models again indicate sedimentation (i.e. moving curves to the left of the 1975 data) whereas they are lower than that of the measured 1990 data. At MSL, both *VR93* (blue-line) and *VR04* have almost similar areas (~7.10 km^2) while it is 8.59 km^2 for *SVR* (red-line). It is generally found that both *VR04* and *VR93* have similar variations between −1.0 m + MSL and +1.0 m + MSL. In contrast, the hypsometry of *SVR* diverges from the other two cases indicating large wet-surface areas. This attributes to a strong sediment export system in the bay under the *SVR* case. Above +1.0 m + MSL, resulting morphology of *VR04* and *VR93* tend to agree with the data, of which *VR04* implies the highest sedimentation at supra-tidal areas.

4.3.2. Sediment volume change in the Ley Bay

Sediment volume change was estimated considering the cell area and the corresponding height with respect to the initial 1984 bathymetry. A decrease in depth indicates sedimentation resulting in a positive volume change and erosion shows a negative volume due to an increase in depth. A net volume change implies whether the system is a sediment importing (positive) or exporting (negative) system. This analysis was also used on the same bay area as in case of the hypsometry.

Sedimentation, erosion and net volume changes are shown in Fig. 13 for the three cases from 1984 to 1990. The highest sedimentation is found under *SVR* (red-line) and *VR93* (blue-line) also shows a similar trend whereas *VR04* (green-line) diverges from the others. The difference between the latter two formulas is about 0.03 Mm^3 while it is about 0.23 Mm^3 with *VR04* implying the lowest sedimentation volume. However, *SVR* has the strongest erosion volume as well. Erosion rates of *VR93* and *VR04* are relatively low and *VR04* shows the lowest values. It is apparent that the Ley Bay has become a sediment exporting system under the three formulas (i.e. net change is negative). The *SVR* formula resulted in the strongest exporting system while the other two show

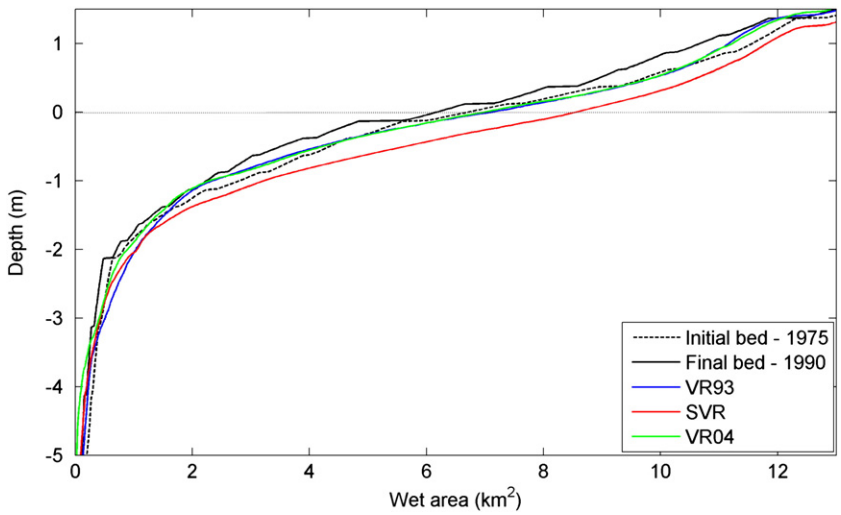

Fig. 12. Ley Bay hypsometry of the final predicted morphologies under different transport formulas compared to the measured data; 1975 bed (black-dash-line), 1990 bed (black-solid-line), Van Rijn, 1993 (blue-line, *VR93*), Soulsby–Van Rijn (red-line, *SVR*) and Van Rijn et al., 2004 (green-line, *VR04*).

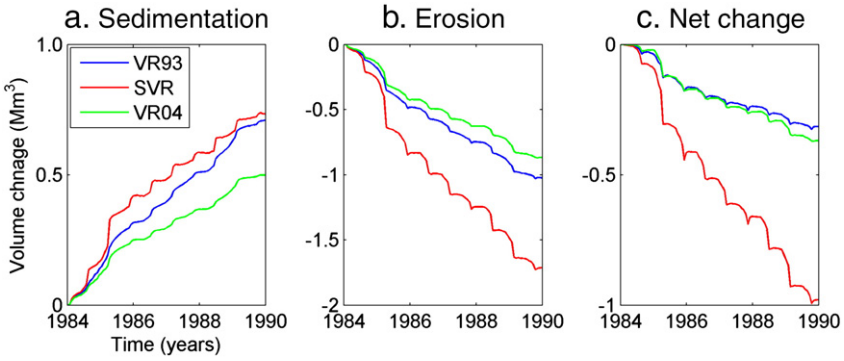

Fig. 13. Sediment volume change in the Ley Bay from 1984 to 1990; sedimentation (a), erosion (b) and net change (c); Van Rijn, 1993 (blue-line, *VR93*), Soulsby–Van Rijn (red-line, *SVR*) and Van Rijn et al., 2004 (green-line,*VR04*).

weak exporting systems. This is however contradicted with the observations which imply a sediment import system.

It is again emphasised that there are only the 1975 and 1990 measured beds available for this study. The Ley Bay evolution shows a sediment import system with respect to these two beds. Such a sediment system is still possible if there is a strong sediment import from 1975 to 1984 (*Stage 1*) and a weak sediment export from 1984 to 1990 (*Stage 2*) as found with the model predictions. Furthermore, the schematised wave climate consists of an extreme event (i.e. $H_s = 3.4$ m from NNW, see Table 3). It was observed that during the application of this wave, a strong sediment movement occurred inside the bay. This event might contribute to develop an exporting system in the Ley Bay evolution from 1984 to 1990.

4.3.3. Channel evolution

Channel evolution was analysed in terms of channel area and volume. Channel area is defined as the water surface area in the Ley Bay below the LW level while the volume considers the water volume below this level. Therefore, an increase in the channel area does not necessarily mean an increase in the volume. The channel area indicates the spatial extent of the bay channels and thus higher areas imply an increasingly submerged portion of the bay area.

Fig. 14 shows the estimated channel area (a) and volume (b) for the three transport formulas. In contrast to the previous analyses, each case has a different value at the beginning of the simulation (i.e. predicted 1984 morphology). This is evidence of having a different bed evolution from 1975 to 1984 (*Stage 1*) under each formula. The largest channel area on the 1984 predicted bed is found with *SVR* (~3.4 km^2) while *VR93* and *VR04* have values of 2.1 and 1.7 km^2 respectively. In *Stage 2*, *SVR* shows a slight increase in the channel area while *VR93* indicates a marginal decrease. In contrast, *VR04* has a more or less constant area and it is further found with the channel volume as well. The other two formulas show an increase in volume from 1984 to 1990 such that the volume increase of the *VR93* formula is about twice (0.4 Mm^3) that of the *SVR* formula (0.2 Mm^3). As mentioned earlier, *VR93* has resulted in an increase in the volume while a decrease in the area (i.e. channels become narrow and deep). Channel evolutions imply that each transport formula tends to develop unique channel configurations in the Ley Bay.

4.3.4. Tidal flat evolution

Tidal flats are defined as shoal areas in between LW and HW in the Ley Bay. Flat areas indicate the plane surface area of these shoals and the volume is a measure of sediment amount remained there.

The resulting tidal flat area (a) and volume (b) during the evolution in *Stage 2* under the three formulas are shown in Fig. 15. As found in the channel analysis, each formula shows a different value of the initial bed (1984) based on the evolution in *Stage 1*. The resulting flat area of *VR04* shows a marginal increase (~0.03 Mm^3). In the case of *VR93*, the flat area increases up until about 1988 and then decreases. *SVR* generally has a decreasing trend during the evolution. All formulas have resulted in a decrease in the flat volume. The highest volume loss (~0.55 Mm^3) is shown in the *SVR* case and it is about 0.39 and 0.21 Mm^3 in the *VR93* and *VR04* cases respectively. Having a strong decrease of flat volume (i.e. losing sediment from the shoals) and increase in channel volume again imply a strong sediment exporting system (i.e. the *SVR* case).

A summary of the previous two analyses is given in the Table 6 comparison to the parameters of the 1975 and 1990 measured beds.

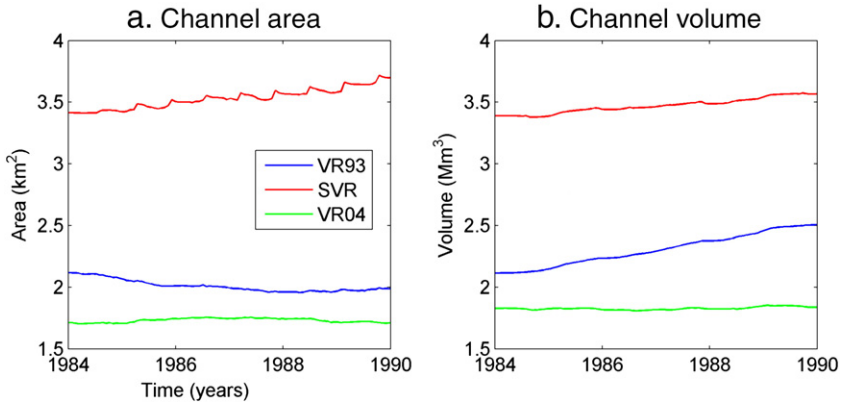

Fig. 14. Channel evolution in the Ley Bay from 1984 to 1990; channel area (a) and channel volume (b); Van Rijn, 1993 (blue-line, *VR93*), Soulsby–Van Rijn (red-line, *SVR*) and Van Rijn et al., 2004 (green-line, *VR04*).

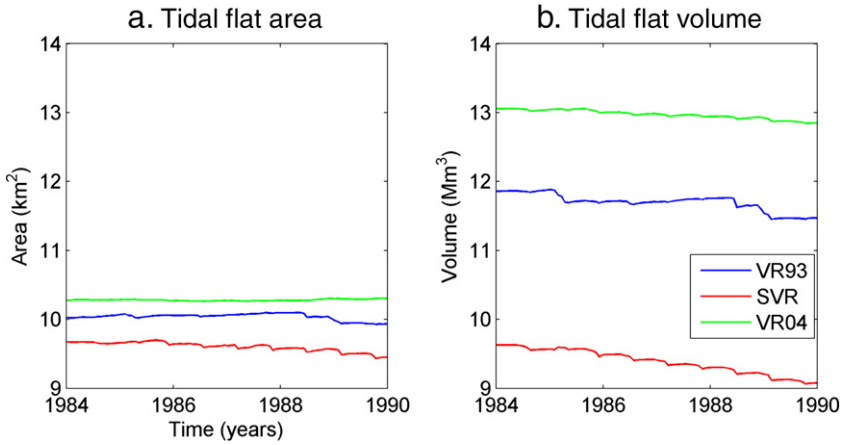

Fig. 15. Tidal flat evolution in the Ley Bay from 1984 to 1990; tidal flat area (a) and tidal flat volume (b); Van Rijn, 1993 (blue-line, *VR93*), Soulsby–Van Rijn (red-line, *SVR*) and Van Rijn et al., 2004 (green-line, *VR04*).

Data indicate a decrease in both channel and tidal flats. It is noted that the overall change of the above parameters decreases due to the implementation of the peninsula though the sedimentation within the Ley Bay is increased. Resulting evolutions show the highest channel area (3.70 km^2) and volume (3.57 Mm^3) under the *SVR* formula. The corresponding lowest values are 1.71 km^2 and 1.84 Mm^3 under *VR04* while they are 1.37 km^2 and 1.43 Mm^3 in the 1990 data. Therefore, the predicted channel evolution of *VR04* has a better agreement with the data compared to the other two formulas. In the case of the tidal flat evolution, the highest tidal flat area (10.31 km^2) and volume (12.85 Mm^3) are obtained in *VR04*. The values of the 1990 data are 10.04 km^2 and 14.79 Mm^3 respectively. Thus, the tidal flat evolution of the *VR04* formula also shows a relatively higher agreement with the data rather than the other two cases. Accordingly, the predicted Ley Bay morphology of the *VR04* formula agrees more with the 1990 data compared to the predictions of *VR93* and *SVR*.

5. Discussion

The morphological evolution of the Ley Bay area is generally analysed based on the measured topographies (Homeier et al., 2010; Knaack et al., 2003). Therefore, applying a numerical model to investigate the decadal evolution is a contemporary approach to hindcast and forecast the morphological changes of a tidal basin system in this area. For the first time, Dissanayake et al. (2012b) described a 2DH numerical model to hindcast the Ley Bay evolution from 1975 to 1990. However, the resulting evolution indicated a number of limitations due to imposing tidal boundary forcings only. Further, they have emphasised the requirement to include both tidal and wave boundaries in order to enhance the sediment distribution inside the bay and then the model predictions. Following these recommendations, the present study simulated the Ley Bay evolution applying both tidal and wave boundary forcings.

Table 6
Comparison of channel and tidal flat parameters in predicted 1990 beds under different transport formulas and measured 1990 data.

Source		Channels		Tidal flats	
		Area (km^2)	Volume (Mm^3)	Area (km^2)	Volume (Mm^3)
Data	1975	1.45	1.63	10.25	15.44
	1990	1.37	1.43	10.04	14.79
1990 model prediction	*VR93*	2.00	2.51	9.94	11.47
	SVR	3.70	3.57	9.45	9.08
	VR04	1.71	1.84	10.31	12.85

Model simulations used a highly schematised wave climate consisting of four wave conditions of which one has an extreme wave height (H_s = 3.4 m, see Section 3.2.2.2). During the evolution, it was observed that a strong sediment transport occurs towards the bay boundaries within this event. This might lead one to underpredict the Ley Bay evolution.

Application of the three sediment transport formulas (*VR93*, *SVR* and *VR04*) showed their sensitivities to the Ley Bay evolution. These formulas mainly differ such that the second formula computes the total load while the other two estimate both suspended and bed loads separately. Section 3.1.1 described the implementation of wave effects in these formulas, which basically enhance the bed shear stress and turbulent mixing leading to an increase in the transport rates. All three cases used a similar approach to compute the cohesive transport (Partheniades' and Krone's formulas). Therefore, different transport patterns mainly ensued due to the different estimation of non-cohesive transports. In conventional non-cohesive sediment transport formulas (e.g. *VR93*, *SVR*), a predefined bed roughness value is employed to estimate the sediment mobility. However, the novelty approach adopted in the *VR04* formula uses the bed roughness predictors to define the roughness value based on the existing hydrolic conditions. Accordingly, the model grid nodes are assigned with spatial and temporal varying bed roughness values which result in more realistic estimation of the sediment transport rates and in turn the morphological evolution. The resulting 1990 morphology under the *VR04* formula shows the highest resemblance with the data (e.g. *BSS* > 0.15) compared to that of the other two transport formulas (*VR93* and *SVR*). Our analysis has shown that the novelty implementation of the bed roughness values in the *VR04* formula results in a more realistic estimation of the sediment transport and then the morphological changes in the Ley Bay and therefore it is recommended for the future studies in this area.

It is noted that the morphological simulation (from 1975 to 1990) was undertaken in two phases, *Stage 1* and *2*, due to the construction of the *Leyhoern* peninsula in 1984. However, there is no measured bathymetric information corresponding to the 1984 peninsula configuration. Therefore, the implementation of the peninsula was entirely based on the 1990 measured data. Such an approach could lead one to underestimate the model predictions (i.e. slight decrease of *BSS* values, see Fig. 11) because the surrounding area of the peninsula might not properly be implemented as in the nature (e.g. it is expected dumping sediment around the peninsula due to deepening of the enclosed area of the peninsula). Therefore, the newly included area is first adjusted on the predicted 1984 morphology during the *Stage 2* simulation. Routine dredging/dumping activities of the bay channels (i.e. facilitating inland drainage and navigation) prior to the construction of the peninsula were also not included into the model due to very sparse

data and that further contributes to the underestimation of the model predictions.

The predicted 1990 morphology of the *VR04* formula shows a reasonable comparison with the 1990 data and thus its temporal evolution can be used to describe the dominant physical processes of the Ley Bay morphological changes. Prior to the peninsula construction (from 1975 to 1984), tidal currents in combination with wave generated currents bring sediment into the Ley Bay leading to the closure of both the Greetsieler and Norder Außentief channels (see Fig. 1). This sediment supply is expected to partly interrupt (i.e. hindering easterly currents) after the peninsula construction (from 1984 to 1990) and then results in sedimentation at the western-foot of the peninsula (see Fig. 7e). Further, the velocity pattern is converged and increased along the Norderley channel (at the north of the peninsula). Therefore, this channel becomes pronounced (see Fig. 7b and e) and provides more sediment towards the Ley Bay. At the bay entrance, easterly velocity diverges and further combines with the velocities reaching from the north. However, the velocity field still has the easterly momentum leading to the development of the easterly bay channel (i.e. Norder Außentief) while resulting in sedimentation in the southern channel (i.e. Greetsieler) (see Figs. 7b and e, 8a and d). Sedimentation areas in the middle of the bay and along the channel banks are not well reproduced by the model (Fig. 8a and d). As discussed earlier, this is mainly due to not implementing the undertaken dredging/dumping activities in the model simulations.

The present model setup (under *VR04*) provides sufficient understanding of the system behaviour due to the implementation of the peninsula and therefore is currently employed to forecast the Ley Bay evolution under different climate change driven future sea level rise scenarios.

6. Conclusions

An anthropogenic effect (i.e. construction of a peninsula) on a tidal basin evolution was investigated using the state-of-the-art Delft3D numerical model in order to understand the potential physical impacts. The study area is the Ley Bay in the East Frisian Wadden Sea. The model simulations spanned 15 years (from 1975 to 1990) under two stages and were forced by tidal and wave boundary forcings. Initial bed sediment composition was adopted from the previous study of Dissanayake et al. (2012b). The sensitivity of the Ley Bay evolution was investigated under three transport formulas (Van Rijn et al., 1993 — *VR93*; Soulsby, 1997 — (Soulsby–Van Rijn) *SVR* and Van Rijn et al., 2004 — *VR04*).

Offshore generated tides and waves were transformed to the model boundaries employing nested modelling approaches. Wave boundaries used a statistically schematised wave climate which consists of four conditions based on the relative contribution of each wave condition to the overall bed level change in the Ley Bay.

Stage 1 extends from 1975 to 1984. In *Stage 2* (from 1984 to 1990), the initial bathymetry used the predicted 1984 morphology of *Stage 1* and the extracted peninsula configuration from the 1990 measured data due to very sparse data (i.e. only 1975 and 1990 measured bathymetries are available). Analysis was undertaken based on the evolution in the second stage to understand the impact of the peninsula on the Ley Bay morphology.

In the visual comparison, the predicted bed evolution of *VR04* appears to have the highest resemblance with the 1990 data (i.e. channel/shoal and erosion/sedimentation patterns). The results of the statistical comparison showed that both *VR93* and *SVR* poorly agree while the *VR04* has reasonable agreement with the data. Quantitative comparison clearly indicated different evolutions under each formula and sediment exporting systems from the Ley Bay in all cases. The strongest sediment export was observed under *SVR*. It was generally found that *VR93* and *VR04* tend to show similar pattern of evolution (i.e. hypsometry, channels, tidal flats). The lowest channel and the highest tidal flat evolution were obtained in *VR04* implying the maximum sediment import into the bay. In this case, the predicted values of these two parameters are only about 17% different from the data. These results could further be improved if the undertaken dredging/dumping activities were implemented into the model. Temporal evolution of the Ley Bay area as approximated here provides a better insight of the potential physical impacts due to the construction of the peninsula and the governing processes of the sediment budget in the Ley Bay. The present model setup (under *VR04*) provides sufficient understanding of the morphological changes and therefore is further employed to investigate the Ley Bay evolution under the climate change driven future sea level rise scenarios.

Acknowledgements

The work presented in this paper was carried out under the project of 'Veränderliches Küstenklima — Evaluierung von Anpassungsstrategien im Küstenschutz (A-KÜST: Changing Coastal Climate — Evaluation of Adaption Strategies for Coastal Protection)' as a part of 'Klimafolgenforschung Szenarien für die Klimaanpassung (KLIFF: Climate Impact Research for Adaption)' funded by the Lower Saxon State Ministry for Science and Culture, Germany.

References

Dastgheib, A., 2012. Long-term Process-based Morphological Modelling of Large Tidal Basins. PhD thesis UNESCO-IHE Institute for Water Education978-1-138-00022-3 (http://repository.tudelft.nl/view/ir/uuid%3A9e12cde6-e127-4e5a-aea5-e57fcb6b8a32/).

Dastgheib, A., Roelvink, J.A., Wang, Z.B., 2008. Long-term process-based morphological modelling of the Marsdiep Tidal Basin. Mar. Geol. 256, 90–100.

Delft3D FLOW user manual http://passthrough.fw-notify.net/static/944019/downloader.js.

Dissanayake, D.M.P.K., 2011. Modelling Morphological Response of Large Tidal Inlet Basin Systems to Sea Level Rise. PhD Thesis UNESCO-IHE Institute for Water Education 978-0-415-62100-7 (http://repository.tudelft.nl/view/ir/uuid%3A59341c96-b5d2-49bf-bdd7-18988e0bed29/).

Dissanayake, D.M.P.K., Roelvink, J.A., Van der Wegen, M., 2009. Modelled channel pattern in schematised tidal inlet. Coast. Eng. 56, 1069–1083.

Dissanayake, D.M.P.K., Ranasinghe, R., Roelvink, J.A., 2012a. The morphological response of large tidal inlet/basin systems to relative sea level rise. Climate Chang. http://dx.doi.org/10.1007/s 10584-012-0402-z.

Dissanayake, D.M.P.K., Wurpts, A., Miani, M., Knaack, H., Niemeyer, H.D., Roelvink, J.A., 2012b. Modelling morphodynamic response of a tidal basin to an anthropogenic effect: Ley Bay, East Frisian Wadden Sea — applying tidal forcing only and different sediment fractions. Coast. Eng. 67, 14–28.

Elias, E., 2006. Morphodynamics of Texel Inlet. PhD Thesis IOS Pres1-58603-676-9 (Technical University of Delft).

Elias, E., Stive, M.J.F., Bonekamp, J.G., Cleveringa, J., 2003. Tidal inlet dynamics in response to human intervention. Coast. Eng. 45 (4), 629–658.

Galappatti, R., 1983. A depth integrated model for suspended transport. Report 83-7, Communications on Hydraulics. Department of Civil Engineering, Delft University of Technology, The Netherlands.

Hartung, W., 1983. Die Leybucht (Ostfriesland) — Probleme ihrer Erhalttung als Naturschutzgebiet. Neues Archiv f. Niedersachsen. Bd. 32, H. 4. Göttingen 355–387 (in Deutsch).

Hayes, M.O., 1979. Barrier Island Morphology as a Function of Tidal and Wave Regime, in Proceedings of the Coastal Symposium of Barrier Islands. In: Leatherman, S.P. (Ed.), Academic Press, New York, pp. 1–28.

Herman, A., Kaiser, R., Niemeyer, H.D., 2007. Modelling of a medium-term dynamics in a shallow tidal sea, based on combined physical and neural network methods. Ocean Model. 17, 277–299.

Homeier, H., 1969. Der Gestaltenwandel der Ostfriesischen Küste im Laufe der Jahrhunderte — Ein Jahrtausend ostfriesischer Deichgeschichte. In: Ohling, H. (Ed.), Ostfriesland im Schutz des Deiches. 2. Deichacht Krummhörn, Pewsum, pp. 3–75 (in Deutsch).

Homeier, H., Stephan, H.J., Niemeyer, H.D., 2010. Historisches Kartenwerk Niedersächsische Küste der Forschungsstelle Küste, Niedersächsischer Landesbetrieb für Wasserwirtschaft, Küsten- und Naturschutz (NLWKN), Geschäftsbereich Gewässerbewirtschaftung und Flussgebietsmanagement (in Deutsch).

Knaack, H., Niemeyer, H.D., 2001. Morphodynamische Gleichgewichtszustände in der Leybucht zwischen 1960 und 1999, Dienstbericht. Niedersächsisches Landesamt für Ökologie, Forschungsstelle Küste, Norderney (in Deutsch).

Knaack, H., Kaiser, R., Niemeyer, H.D., 2003. Mathematische Modellierung von Tiden in der Leybucht, Dienstbericht. Niedersächsisches Landesamt für Ökologie, Forschungsstelle Küste, Norderney (in Deutsch).

Leendertse, J.J., 1987. A three-dimensional alternating direction implicit model with iterative fourth order dissipative non-linear advection terms. WD-333-NETH.Rijkswaterstaat, The Netherands.

Lesser, G.R., Roelvink, J.A., Van Kester, J.A.T.M., Stelling, G.S., 2004. Development and validation of a three-dimensional morphological model. Coast. Eng. 51, 883–915.

Niemeyer, H.D., 1984. Hydrographische Untersuchungen in der Leybucht zum Bauvorhaben Leyhörn. Jahresbericht 1983 Forschungsstelle f. Insel- u. Küstenschutz. 35, pp. 61–98 (Norderney, in Deutsch).
Niemeyer, H.D., 1991. Case study Ley Bay, an alternative to traditional enclosure. Proc. 3rd Conf. on Coastal and Port Engineering in Developing Countries (COPEDEC). Mumbasa, Kenya.
Niemeyer, H.D., 1994. Hydrodynamical investigations for coastal protections measures. Case Study Ley Bay. Proc. Int. Conf. Hydrodyn.'94. Wuxi, China.
Partheniades, E., 1965. Erosion and deposition of cohesive soils. J. Hydraul. Div. ASCE 91 (HY1).
Roelvink, J.A., 2006. Coastal morphodynamic evolution techniques. Coast. Eng. 53, 277–287.
Soulsby, R., 1997. Dynamics of Marine Sands — A Manual for Practical Applications. Thomas Telford Publications 182–184.
Stelling, G.S., 1984. On the construction of computational methods for shallow water flow problem. Rijkswaterstaat Communications, vol. 35. Governing printing Office, The Hague, The Netherlands.
Stelling, G.S., Leendertse, J.J., 1991. Approximation of convective processes by cyclic AOI methods. Proceeding of the 2nd ASCE Conference on Estuarine and Coastal Modelling, Tampa. ASCE, New York, pp. 771–782.
Stive, M.J.F., Roelvink, J.A., De Vriend, H.J., 1990. Large-scale coastal evolution concept. Proc. 22nd Int. Conf. on Coastal Engineering. ASCE, New York.
Sutherland, J., Peet, A.H., Soulsby, R.L., 2004. Evaluating the performance of morphological models. Coast. Eng. 51, 917–939.
Thijsse, J.T., 1972. Een halve Zuider Zeewerken 1920–1970. Tjeenk Willink, Groningen (in Dutch).
Van der Wegen, M., 2010. Modelling Morphodynamic Evolution in Alluvial Estuaries. PhD Thesis UNESCO-IHE Institute for Water Education978-0-415-59274-1 (http://repository.tudelft.nl/search/ir/?q=title%3A%22Modeling%20morphodynamic%20evolution%20in%20alluvial%20estuaries%22).
Van der Wegen, M., Roelvink, J.A., 2008. Long-term morphodynamic evolution of a tidal embayment using a two-dimensional, process-based model. J. Geophys. Res. 113. http://dx.doi.org/10.1029/2006JC003983 (C03016).
Van der Wegen, M., Roelvink, J.A., De Ronde, J., Van der Spek, A., 2008. Long-term Morphodynamic Evolution of the Western Scheldt Estuary, the Netherlands, Using a Process-based Model. COPEDEC VII, Dubai, UAE.
Van Rijn, L.C., 1993. Principles of Sediment Transport in Rivers, Estuaries and Coastal Seas. AQUA Publications, the Netherlands.
Van Rijn, L.C., Walstra, D.J.R., Van Ormondt, M., 2004. Description of TRANSPOR2004 and Implementation in Delft3D-ONLINE, WL |Delft Hydraulics Report, Z3748.00.
Verboom, G.K., De Ronde, J.G., Van Dijk, R.P., 1992. A fine grid tidal flow and storm surge model of the North Sea. Cont. Shelf Res. 12.